Extended Abstracts of the 2018 International Conference on Solid State Devices and Materials, Tokyo, 2018, pp825-826

Grain-Boundary-Limited Polycrystalline-Silicon Mobility with Negative Temperature Dependence ~ Modeling of Carrier Conduction through Grain-Boundary Traps Based on Trap-Assisted Tunneling ~

Michiru Hogyoku, Takashi Izumida, Hiroyoshi Tanimoto, Nobutoshi Aoki, and Seiji Onoue
Institute of Memory Technology Research & Development, Toshiba Memory Corporation
1, Komukai-Toshiba-cho, Saiwai-ku, Kawasaki 212-8583, Japan
Tel: +81-503-190-8169, E-mail: michiru.hogyoku@toshiba.co.jp

Abstract

Based on the thermionic emission (TE) theory, the so-called Seto's model explains that the grain-boundary(GB)-limited carrier mobility in polycrystalline-silicon (poly-Si) is dependent positively on a temperature. Although this model is widely accepted as a standard model of the GB-limited mobility in poly-Si, many experiments support extremely-weak or negative temperature dependence. In this report, we have formulated carrier conduction through GB traps by utilizing the so-called trap-assisted tunneling (TAT) model based on the non-radiative multi-phonon transition theory. Self-consistent calculation has revealed that in contrast to the Seto's model, our novel model can reproduce the GB-limited mobility dependent negatively on a temperature. From the viewpoint of consistency with experiments, our novel model seems more appropriate than the Seto's model.

1. Introduction

The Seto's model [1], which is based on the TE theory, has been widely accepted as a standard model of the GB-limited carrier mobility in poly-Si [2, 3]. It has been already known that because a GB barrier is not very high in poly-Si films, the quantum-mechanical tunneling through the GB barrier is not significant compared with TE [4, 5]. The most essential consequence of the Seto's model is that the GB-limited mobility is temperature-activated and dependent positively on a temperature. Therefore, when the measured mobility shows extremely-weak or negative temperature dependence, we do not usually consider the mobility limited by GBs but that controlled by in-grain or MOS-interface defects instead [3]. We note that a low GB barrier energy less than the thermal energy (***kT***), which can reproduce the GB-limited mobility dependent negatively on a temperature [1], tends to overestimate a value of that mobility (see Sec. 3).

The circumstances explained above seem to suggest that the GB-limited mobility proportional to a grain size cannot be interpreted consistently with negative temperature dependence. This inconsistency will be, however, dissolved if we have developed a ***novel*** GB-limited mobility model that can reproduce negative temperature dependence. In this report, we formulate carrier conduction through GB traps by utilizing the TAT model [6 - 11], and then reveal that our model reproduces extremely-weak temperature dependence of the GB-limited mobility.

2. Grain-Boundary Modeling Based on Trap-Assisted Tunneling

In this section, carrier conduction through GB traps is formulated by utilizing the TAT model. In general, each localized electronic state is stabilized by the self-trapping mechanism, namely by local polarization due to lattice displacement [12]. Supposing the lattice displacement, the TAT model considers non-radiative multi-phonon transition [12]. Examples to which the TAT model has been applied extend over various kinds of simulation including SILC [6, 7] and RTN [8 - 10] as well as MONOS [11].

According to Refs. [1, 2], trapped charges on a GB have been expected to induce a parabolic potential barrier. Therefore, we can expect that the TAT model for GB traps is derived by replacing a trapezoidal potential barrier usually assumed in the TAT model for SILC [6, 7] with a parabolic one (see Fig. 1). A potential barrier induced by trapped charges on a GB ($\boldsymbol{Q_t}$ [1/cm^2]) is schematically shown in Fig. 2. Figure 2 also shows equations for lengths and heights of the potential barrier, as well as an equation for an applied bias ($\boldsymbol{V_a}$ [V]) between anode and cathode sides of the potential barrier. All equations shown in Fig. 2 have been derived by using the literatures [1, 2] as reference. We note that a grain size of poly-Si is assumed to be larger than a sum of barrier lengths for both cathode and anode sides, namely $\boldsymbol{Q_t} / \boldsymbol{N}$ where $\boldsymbol{N}$ [1/cm^3] is a volume concentration of free carriers (see Sec. 3). In Fig. 3, energies of trapped carriers on a GB and of de-trapped carriers are shown on a parabolic energy profile of the conduction band edge for a cathode or anode side ($\boldsymbol{E_C(x)}$ [eV]). An energy difference between de-trapped and trapped carriers is attributed to the multi-phonon emission or absorption ($\boldsymbol{p\hbar\omega}$ [eV]) during carrier-trapping. $\boldsymbol{p}$ is a number of phonons emitted during carrier-trapping (negative $\boldsymbol{p}$ indicates phonon absorption). $\boldsymbol{\hbar\omega}$ [eV] is a single phonon energy typical for displaced lattice-vibration-modes.

We have formulated TAT rates for capture and emission of carriers, based on following two concepts: A short-range interaction [9] for the transition matrix element of carriers, originally proposed by Lundstrom and Svensson [13]; simplified statistics [7, 8, 10] for energies of tunneling carriers, originally introduced by Herrmann and Schenk [6]. Assuming large grains, those rates have been expressed as

$$\tau_{c,y}^{-1} = \frac{2\pi}{\hbar}\cdot 8\pi\Phi_t^2 r_t^3 \cdot \frac{\sqrt{2}}{\pi^2\hbar^3} m_{dos}^{3/2} \cdot \sum_p^{E\geq 0}\Big[\sqrt{E}\cdot f_{FD}(E,E_F,kT) \cdot T_{WKB}(x_1,x_2)\cdot P_{MP}(p,S,\hbar\omega,kT)\Big],$$

$$\tau_{e,y}^{-1} = \frac{2\pi}{\hbar}\cdot 8\pi\Phi_t^2 r_t^3 \cdot \frac{\sqrt{2}}{\pi^2\hbar^3} m_{dos}^{3/2} \cdot \sum_p^{E\geq 0}\Big[\sqrt{E}\cdot\big[1-f_{FD}(E,E_F,kT)\big] \cdot T_{WKB}(x_1,x_2)\cdot P_{MP}(-p,S,\hbar\omega,kT)\Big], \quad (1)$$

$$\Big[r_t = \hbar\Big/\sqrt{2m_{tun}\Phi_t}\,, \qquad E = E_C(x_1)\Big]$$

where "$\boldsymbol{y}$" is "$\boldsymbol{c}$" (cathode) or "$\boldsymbol{a}$" (anode) and $\boldsymbol{\tau_{c,y}}^{-1}$ and $\boldsymbol{\tau_{e,y}}^{-1}$ [1/s] are capture and emission rates of carriers by GB traps, respectively. $\boldsymbol{r_t}$ is a localization length of GB traps, $\boldsymbol{m_{dos}}$ is the density-of-states effective-mass for a poly-Si grain, $\boldsymbol{f_{FD}}()$ is the Fermi-Dirac distribution function, and $\boldsymbol{E_F}$ is the Fermi level of carriers in a grain whose concentration is $\boldsymbol{N}$. $\boldsymbol{P_{MP}}()$ is the multi-phonon transition probability under the Condon approximation (see Eq. (6.66) of Ref. [12]), $\boldsymbol{S}$ is the Huang-Rhys factor (see Sec. 6.1 of Ref. [12]), and $\boldsymbol{m_{tun}}$ is the tunneling mass of carriers in a grain. See Fig. 3 for parameters such as $\boldsymbol{\Phi_t}$, $\boldsymbol{x_1}$, and $\boldsymbol{x_2}$.

According to Eqs. (6 - 9) of Ref. [5], the tunneling probability of carriers across a parabolic GB barrier, denoted by $\boldsymbol{T_{WKB}}()$ in Eqs. (1), has been expressed as

$$T_{WKB} = \exp\left[-\sqrt{\frac{q^2 m_{tun} N}{\hbar^2\varepsilon}}\left[x_2\sqrt{x_2^2-x_1^2} - x_1^2\cdot\ln\left\{\left(x_2+\sqrt{x_2^2-x_1^2}\right)\Big/x_1\right\}\right]\right]. \quad (2)$$

Using Eqs. (8) and (15) of the literature [7] as reference, a carrier occupancy of GB traps ($\boldsymbol{f_t}$) and a TAT current density through GB traps ($\boldsymbol{J_{TAT}}$ [C/cm^2/s]) have been expressed at a steady-state as

$$f_t = \frac{\tau_{c,c}^{-1}+\tau_{c,a}^{-1}}{\tau_{c,c}^{-1}+\tau_{c,a}^{-1}+\tau_{e,c}^{-1}+\tau_{e,a}^{-1}}, \qquad J_{TAT} = qN_t\left[(1-f_t)\tau_{c,c}^{-1} - f_t\tau_{e,c}^{-1}\right], \quad (3)$$

where $\boldsymbol{N_t}$ [1/cm^2] is a surface concentration of GB traps.

3. Self-consistent Calculation and Results

Using equations shown in Figs. 2 and 3, $\boldsymbol{E_C(x)}$ for both cathode and anode sides can be derived from $\boldsymbol{Q_t}$. On the other hand, $\boldsymbol{Q_t}$ (= $\boldsymbol{f_t N_t}$) can be calculated from $\boldsymbol{E_C(x)}$ for the both sides, according to Eqs. (1), (2), and (3). In order to self-consistently carry out those derivation and calculation, we have developed the EXCEL program based on a scheme shown in Fig. 4.

We then tried to confirm that the above program reproduces experimental temperature dependence of the electron mobility in poly-Si shown in Ref. [3]. Parameters used in self-consistent calculation are summarized in Table I. Reference [3] has reported that a median size of poly-Si grains is approximately 0.8 μm. We note that according to preceding calculation for the 0.8 μm grain size, a low GB potential barrier

less than kT/q yields the unphysical GB-limited mobility larger than 2000 [cm^2/V/s]. Figure 5 shows calculation results of temperature dependence of the electron mobility for total currents including both TAT and TE. Calculation results for a TE current only are also shown in Fig. 5 as reference. In contrast to strong positive temperature dependence of TE, the total electron mobility dominated by TAT shows extremely-weak negative temperature dependence, which has been attributed to the inverted region effect of the so-called Marcus theory [14]. In Fig. 5, N is supposed to be 2 x 10^{18} [1/cm^3]. If an induced channel thickness [2] is assumed to be 5 nm, the corresponding surface concentration (N_s [1/cm^2]) is estimated to be 1 x 10^{12} [1/cm^2]. One can see that extremely-weak temperature dependence of the experimental electron mobility about 50 [cm^2/V/s], which has been shown for N_s = 1 x 10^{12} [1/cm^2] in Ref. [3], is comparable with our calculation results shown for N = 2 x 10^{18} [1/cm^3] in Fig. 5. We note that the 0.8 μm grain size is larger than the maximum Q_t / N, namely 30 nm.

4. Conclusions

Utilizing the TAT model based on the non-radiative multi-phonon transition theory, we have formulated carrier conduction through GB traps. Self-consistent calculation has revealed that in contrast to the conventional Seto's model based on the TE theory, our novel model can reproduce the GB-limited mobility dependent negatively on a temperature. From the viewpoint of consistency with experiments, our novel model seems more appropriate than the Seto's model.

References

[1] J. Y. W. Seto, J. Appl. Phys. **46**, 5247 (1975). [2] J. Levinson et al., J. Appl. Phys. **53**, 1193 (1982). [3] M. Oda et al., Tech. Dig. Int. Electron Devices Meet. 2015, 125. [4] C. H. Seager and G. E. Pike, Appl. Phys. Lett. **35**, 709 (1979). [5] C. H. Seager and G. E. Pike, Appl. Phys. Lett. **40**, 471 (1982). [6] M. Herrmann and A. Schenk, J. Appl. Phys. **77**, 4522 (1995). [7] A. Gehring et al., Microelectron. Reliab. **43**, 1495 (2003). [8] F. Schanovsky et al., J. Comput. Electron. **11**, 218 (2012). [9] M. Zhang and M. Liu, J. Appl. Phys. **113**, 144503 (2013). [10] Y. Higashi et al., IEEE Trans. Electron Devices **61**, 4197 (2014). [11] K. A. Nasyrov et al., J. Appl. Phys. **105**, 123709 (2009). [12] B. K. Ridley, Quantum Processes in Semiconductors, 4th ed., Clarendon, Oxford, 1999, Chapter 6. [13] I. Lundstrom and C. Svensson, J. Appl. Phys. **43**, 5045 (1972). [14] R. A. Marcus, Rev. Mod. Phys. **65**, 599 (1993).

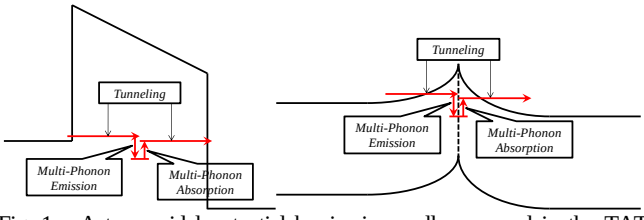

Fig. 1. A trapezoidal potential barrier is usually assumed in the TAT model for SILC [6, 7], as schematically shown in the left side. On the other hand, a parabolic potential barrier is expected for TAT carrier conduction through GB traps, as shown in the right side.

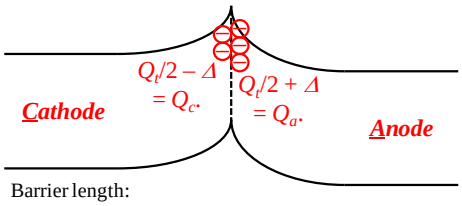

Barrier length:
Q_c / N, Q_a / N.
Potential barrier height:
$q\,Q_c^2 / (2\,\varepsilon\,N)$, $q\,Q_a^2 / (2\,\varepsilon\,N)$.
Applied bias between cathode and anode sides:
$V_a = q\,(Q_a^2 - Q_c^2) / (2\,\varepsilon\,N)$.
$[\,\Delta = \varepsilon N\,V_a / (q\,Q_t)\,]$

Fig. 2. Energy-band-bending due to trapped charges on a GB (Q_t [1/cm^2]) is schematically shown in the upper figure. Below that figure, we also list equations concerning barriers of both cathode and anode sides. Q_c and Q_a [1/cm^2] are surface concentrations of GB-trapped-charges that should be assigned to cathode and anode sides, respectively. q [C] and ε [C/V/cm] are the elementary electronic charge and the permittivity in poly-Si, respectively. A difference between Q_a and Q_c, namely 2Δ [1/cm^2], is related to V_a.

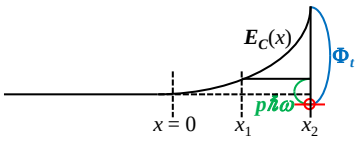

$$x_2 = Q_y / N \quad (0 \le x_1 \le x_2, \quad Q_y = Q_c \text{ or } Q_a),$$

$$E_C(x) = \frac{q^2 N}{2\varepsilon} x^2 \quad \left[E_C(x_1) = \frac{q^2 N}{2\varepsilon} x_1^2, \quad E_C(x_2) = \frac{q^2 N}{2\varepsilon} x_2^2 \right],$$

$$E_C(x_1) - \left[E_C(x_2) - \Phi_t \right] = p\hbar\omega, \quad \Rightarrow \quad x_1 = \sqrt{x_2^2 - \frac{2\varepsilon}{q^2 N}(\Phi_t - p\hbar\omega)}.$$

Fig. 3. The upper figure shows $E_c()$ for a cathode or anode side as a parabolic function of x. x_1 [cm] is a position of a classical turning point for de-trapped carriers. x_2 [cm] is a position of a GB, and also a barrier length. Φ_t [eV] is the trap depth. See Fig. 2 for $Q_y = Q_c$ or Q_a. x_1 is related to x_2 and $p\hbar\omega$.

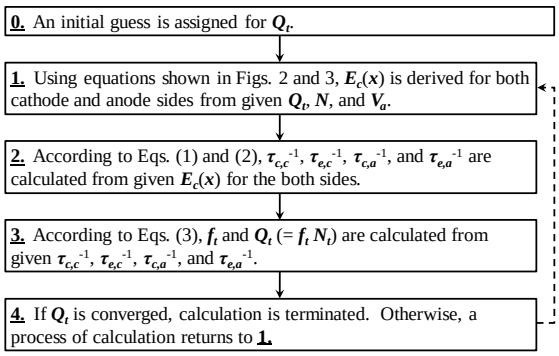

Fig. 4. A scheme is shown for self-consistent calculation of TAT through GB traps.

Trap-Type 1: $\hbar\omega$ = 0.02 eV, Φ_t = 0.315 eV, S = 1, N_t = 2 x 10^{12} cm^{-2}.
Trap-Type 2: $\hbar\omega$ = 0.02 eV, Φ_t = 0.400 eV, S = 2, N_t = 2 x 10^{12} cm^{-2}.
Trap-Type 3: Φ_t ~ 0.5 eV, $N_{fixed\text{-}charges}$ = 2 x 10^{12} cm^{-2}.
ε = 11.7 x ε_0 C/V/cm, m_{dos} = 6$^{2/3}$ x 0.33 m_0, m_{tun} = 0.08 m_0.

Table I. Parameters used in self-consistent calculation are listed. We have assumed three types of GB traps including deep levels, namely "Trap-Type 3". Preceding calculation has ensured that "Trap-Type 3" behaves like fixed charges.

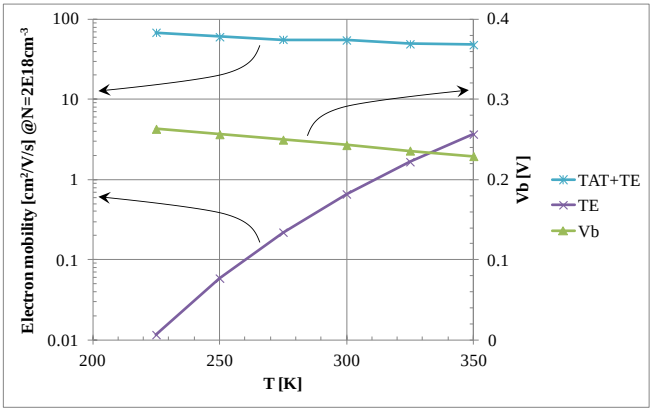

Fig. 5. "TAT+TE" and "TE" indicate the GB-limited electron mobility for total currents and that for a TE current only, respectively. Vb [V], namely a GB potential barrier height measured at a cathode side, is about 10 times larger than kT/q.